

## Fabrication of Poly(vinyl alcohol) Nanofibers by Wire Electrode-Incorporated Electrospinning

Chien-Teng Hsieh<sup>1</sup>, Ching-Wen Lou<sup>2</sup>, Yi-Jun Pan<sup>3</sup>, Chien-Lin Huang<sup>4</sup>, Jia-Horng Lin<sup>5,6,7,8\*</sup>, Zheng-Ian Lin<sup>6</sup>, Yueh-Sheng Chen<sup>9</sup>, and Kun-Chien Chiang<sup>6</sup>

<sup>1</sup>*Department of Fashion Design and Merchandising, Shih Chien University Kaohsiung Campus, Kaohsiung City 84550, Taiwan*

<sup>2</sup>*Institute of Biomedical Engineering and Materials Science, Central Taiwan University of Science and Technology, Taichung City 40601, Taiwan*

<sup>3</sup>*Department of Materials and Textiles, Oriental Institute of Technology, New Taipei City 22061, Taiwan*

<sup>4</sup>*Department of Fiber and Composite Materials, Feng Chia University, Taichung City 40724, Taiwan*

<sup>5</sup>*School of Textiles, Tianjin Polytechnic University, Tianjin 300387, China*

<sup>6</sup>*Laboratory of Fiber Application and Manufacturing, Department of Fiber and Composite Materials, Feng Chia University, Taichung City 40724, Taiwan*

<sup>7</sup>*School of Chinese Medicine, China Medical University, Taichung City 40402, Taiwan*

<sup>8</sup>*Department of Fashion Design, Asia University, Taichung City 41354, Taiwan*

<sup>9</sup>*Department of Biomedical Imaging and Radiological Science, China Medical University, Taichung City 40402, Taiwan*

(Received March 24, 2016; Revised June 19, 2016; Accepted June 23, 2016)

**Abstract:** Wire electrodes for needleless electrospinning consist of stainless steel wires in place of cylinder electrodes. The effects of different numbers of constituent stainless steel wires on the morphology and diameter of polyvinyl alcohol (PVA) fibers are examined. With 1, 2, 3, or 4 stainless steel wires being twisted as wire electrodes, an 8, 10, or 12 wt.% polyvinyl alcohol (PVA) solution is electrospun into PVA nanofibers by using a needleless electrospinning machine. The morphology and diameter of PVA nanofibers is observed by scanning electron microscopy. The combination of the number of stainless steel wires (two), PVA solution (10 wt.%), and the collecting distance (10 cm) results in the finest diameter and an evenly formed fiber morphology. In addition, the nanofibers exhibit a wide range of diameters when electrospun with an electrode consisting of more than two stainless steel wires. Compared with the cylinder electrode, the use of a wire electrode can form nanofibers, which results in a more even morphology.

**Keywords:** Electrospinning, Needleless electrospinning, Wire electrodes, Nanofiber, Polyvinyl alcohol (PVA)

### Introduction

Nanofibers are defined as fibers with diameters of below 1000 nm. Owing to high porosity, high specific surface, and excellent mechanical properties, nanofibers are commonly used as wound dressing, for drug release applications and tissue engineering scaffolds in medicine, as filtration and metal ion adsorption for environmental applications, as well as battery separators and bio-sensors for photoelectric applications [1-6].

Electrospinning was first introduced in 1934 by Formhals, who focused on cellulose acetate by studying the influences of solution properties on fibers that are collected on the collector [7]. This technique involves traditional single-needle electrospinning that induces a high voltage to the needle while the collection end is connected to the ground so as to form an electrical potential difference for electrospinning [8]. However, this traditional electrospinning method results in a low yield of 0.01-0.1 g/h and does not allow for mass production. Needleless electrospinning [9-14], which has

been developed in this decade, does not exhibit the disadvantage of clogging. Thus, this technique shows potential for mass production [15-21].

A study by Yarin *et al.* introduced the magnetic-field-assisted needleless electrospinning, which creates a magnetic liquid at a wave shape in a polymer solution bath. Therefore, the polymer solution above the magnetic liquid forms a jet to facilitate the electrospinning process [22]. Jirsak *et al.* proposed the use of a rotating roller, which allows for slow adherence of the polymer solution; then, the polymer solution over the roller is drawn into a jet. This novel needleless electrospinning method for nanofiber production is being rapidly utilized commercially by Elmarco [23]. Liu *et al.* used nitrogen or an air compressor to create air bubbles over the surface of polymer solutions. Cones that were formed over the bubbles were equivalent to the Taylor cones, which are commonly seen in traditional electrospinning, and allowed for a tremendous amount of jet for electrospinning [24,25]. Wang *et al.* incorporated conical wire coils with electrospinning and found numerous polymer jets over the coils [26]. The group also created a rotating spiral coil to serve as a spinneret, thereby leading to the accomplishment of an original needleless electrospinning approach [27,28]. Forward

\*Corresponding author: jhlin@fcu.edu.tw

*et al.* further used wire electrodes to replace the conventional single needle for electrospinning. As a result of their rotation in the polymer solution bath, numerous spheres were formed on wire electrodes and eventually transformed into jets [29]. Numerous types of needleless electrospinning are available. In particular, the conjunction of wire electrodes in electrospinning, which was invented by Forward *et al.*, requires a relatively smaller threshold voltage, thereby benefiting the production of nanofibers. Recently, there have been more and more studies focusing wire electrodes [29-34]. Thus, a custom-made needleless electrospinning machine was used to attempt to replace cylinder electrodes with a wire electrode, as well as to improve the yields and morphology of nanofibers. Stainless steel wires are used in the hope of adhering polymer solution over their crossing points, thereby manipulating the droplet size and forming a Taylor cone of polymer solution in order to facilitate the electrospinning process. Compared to using a cylinder electrode, using a wire electrode does not easily dissipate the voltage and thus stabilizes the applied high voltage. Moreover, unlike a wire coil electrode, a wire electrode does not have the disadvantage of Taylor cones being concentrated in the wire coil, which allows for more available spinning locations [34]. In this study, the wire electrodes consisting of one, two, three, or four stainless steel (SS) wires are respectively incorporated into the electrospinning process. Additionally, the wired drum nozzle proposed by Elmarco combines many single wires, while ours combines 1 to 4 SS twists as strands to form the same drum nozzle structure [23]. As such, the differences in morphology and nanofiber diameter in relation to the number of SS twists are examined. In addition, PVA features good biodegradability, water soluble, film forming ability, and barrier properties, and has been commonly used in different fields. Accordingly, different concentrations of PVA solutions are selected for the preparation of nano-fibers.

That is, 8, 10, and 12 wt.% PVA solutions are examined in relation to the nanofiber morphology and diameter.

## Experimental

### Materials

Polyvinyl alcohol (PVA, Sigma-Aldrich Co., Ltd., USA) possesses a molecular weight ( $M_w$ ) of 89,000-98,000 and is 99+% hydrolyzed. SS wires (King Metal Fiber Technology Co., Ltd., Taiwan, R.O.C.) were 0.2 mm in diameter.

### Methods

#### *Solution Preparation*

PVA powders are dissolved in deionized water to prepare 8, 10, and 12 wt.% PVA solutions. The solutions are heated and blended using a magnetic stirrer at 90 °C for 6 h.

#### *Custom-Made Electrospinning Machine*

The PVA solutions are measured for viscosity and subsequently electrospun into nanofibers by using a custom-made electrospinning machine, as indicated in Figure 1(a). The electrospinning settings are as follows: high voltage (80 kV), distance of electric field (10, 15, or 20 cm), rotary speed (8 rpm), ambient temperature (25 °C), and relative humidity (55 %). Figure 1(a) is the schematic of the custom-made electrospinning machine. According to Forward *et al.* [29], one, two, three, or four SS wires are twisted into 1-, 2-, 3-, and 4-SS wire electrodes, which are compactly and uniformly formed, as indicated in Figure 2. The corresponding diameter of each wire electrode is 0.2 mm (1-SS), 0.4 mm (2-SS), 0.6 mm (3-SS), and 0.8 mm (4-SS). The cylinder electrode with a diameter of 8 cm (the control group) is shown in Figure 3. The electrospinning procedure is introduced as follows. First, the wire electrode is equipped with the spinneret. The spinneret is affixed to the chucks at both ends and then rotated by a connected pulley, which acts as a result

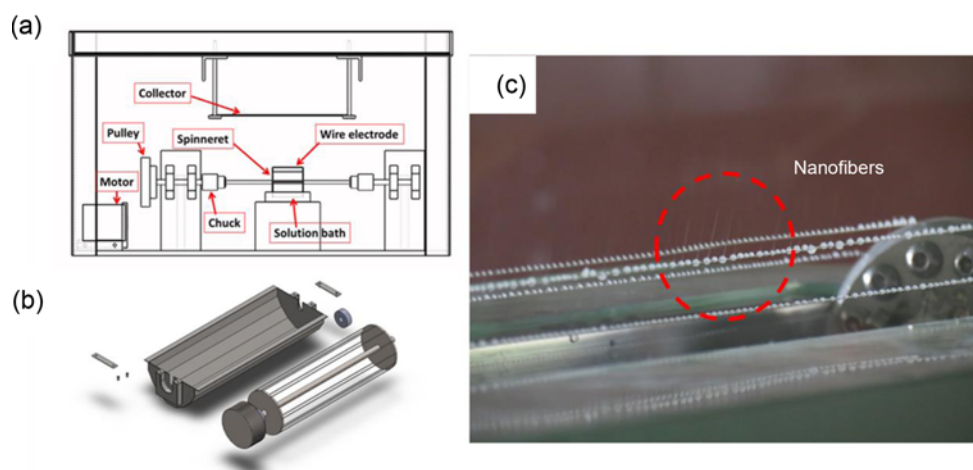


**Figure 1.** Illustrations of (a) the custom-made electrospinning machine, (b) the wire electrode and solution bath, and (c) image of the electrospinning process.

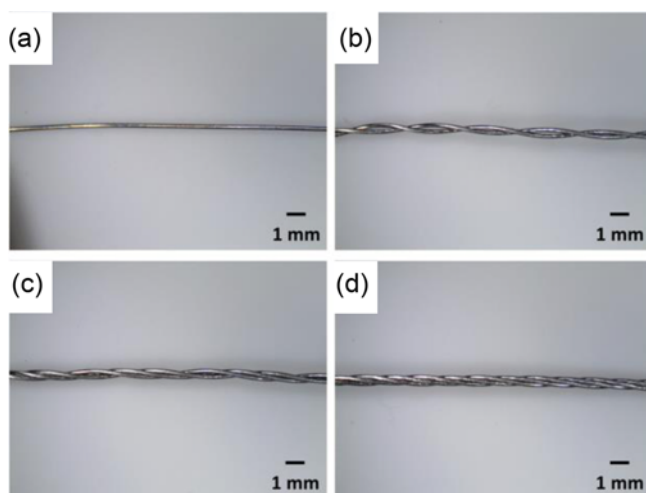


**Figure 2.** Stereomicroscopic images of wire electrodes that are composed by twisting (a) one, (b) two, (c) three, and (d) four SS wires.



**Figure 3.** Image of the cylinder electrode.

**Table 1.** Viscosity of the PVA solution

	PVA 8 wt%	PVA 10 wt%	PVA 12 wt%
Viscosity (cP)	365.6±26.5	489.9±38.2	546.2±21.8

of the dynamic force provided by a motor. Then, the wire electrodes are dipped into the polymer solutions, and the solutions will form spheres due because of surface tension, gravity, and viscosity. High voltage is applied to the wire electrodes, and solution spheres will form Taylor cones and then jets. Finally, the nanofibers are drawn onto the collector. In this study, both wire electrodes and a cylinder electrode are used for electrospinning. The voltage is constant at 80 kV. After the measurement, the threshold voltage for the cylinder electrode is 70 kV, while the threshold voltage for wire electrodes are 78 kV (1-SS), 78 kV (2-SS), 77 kV (3-SS), and 76 kV (4-SS). The cylinder electrode has a significantly

lower threshold voltage than the setting voltage, which is also considered to be responsible for a greater variation in nanofiber diameter. Moreover, Table 2 shows that using a cylinder electrode requires a higher voltage to ensure that the polymer solution completely covers the cylinder, thereby resulting in a loss of voltage and an uneven drawing force for electrospinning. In addition, when PVA solution adheres to the cylinder electrode, it forms a wavy surface that interferes with the evenness of Taylor cones. Thus, the formed nanofibers have a broad range of diameter. Thus, the wire electrodes are more energy-efficient.

## Tests

### Viscosity

PVA solutions are tested for viscosity by using a rotational viscometer (Fungilab, Spain). The concentrations, viscosity, and the morphology of the nanofibers are correlated

### Scanning Electron Microscopy (SEM)

Various nanofibers are placed in an oven at 40 °C for 24 h to remove moisture from the surface. Samples are coated with a thin gold layer, and morphology was observed in conjunction with SEM (S3000N, HITACHI, Japan) under an operating voltage of 10 kV.

### Diameter Analyses

Morphology images obtained from the section of Scanning Electron Microscopy (SEM) are then analyzed with the incorporation of an Image-Pro 6.2 illustration. A total of 100 nanofibers were collected for fiber diameter measurement, and the influences of manufacturing parameters are thereby determined.

## Results and Discussion

### Viscosity of PVA Solutions

The viscosity of PVA solutions is an important parameter in electrospinning, regardless of conventional single-needle electrospinning and needleless electrospinning. The optimal viscosity range for electrospinning demonstrates a significant influence on the morphology of nanofibers [35]. The viscosity of PVA solution is proportional to PVA concentration, and increasing from 365.6 cP to 546.9 cP following the concentration of 8 wt.% to 12 wt.%. PVA is a polymer; higher concentration causes molecular chain movement, and the subsequent chain entanglement eventually results in a distinctive increase in viscosity. This process in turn contributes to variations in morphology from bead-containing to spindle-like; finally, the nanofibers gradually become even [4,36].

### Effect of Cylinder Electrode on Nanofiber Morphology

The SEM images in Figure 4 show the nanofibers, which were produced using a cylinder electrode. The columns refer to the concentration of PVA solution (8, 10, and 12 wt.%), and the rows refer to collecting distance (10, 15, and 20 cm). With a specified 8 wt.% PVA solution, a collecting distance

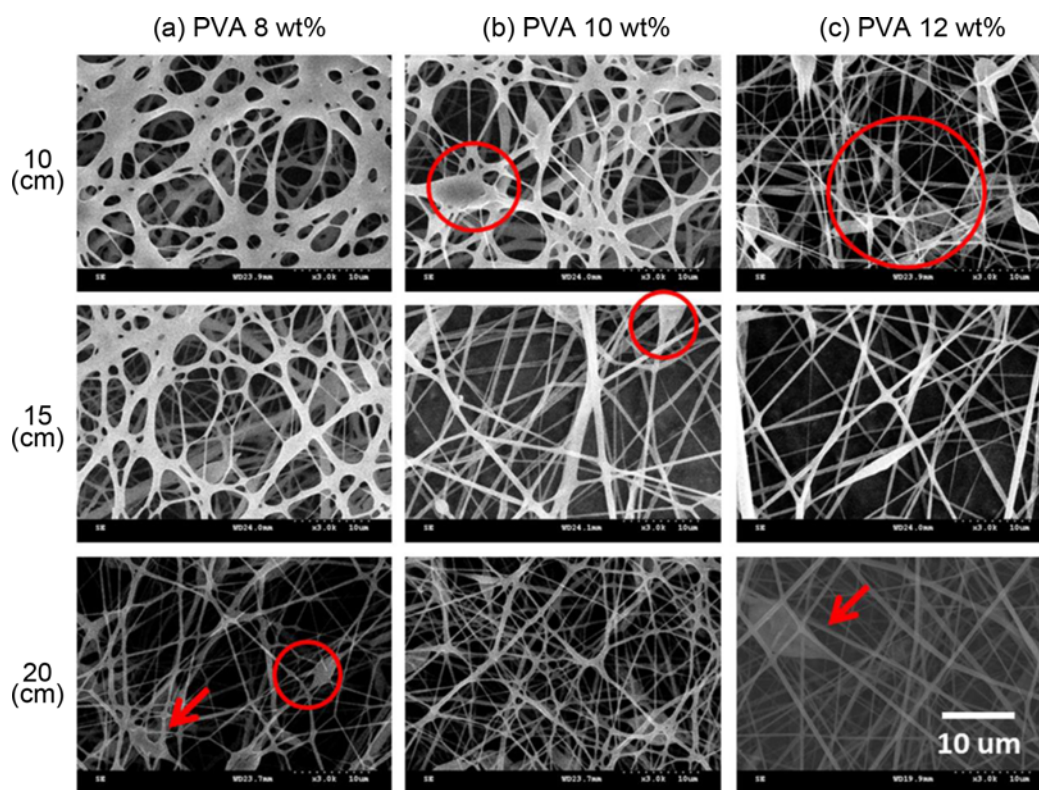


**Figure 4.** SEM images (3000 $\times$ ) of nanofibers that are made using a cylinder electrode. The PVA spinning solutions contain (a) 8, (b) 10, and (c) 12 wt.% concentration. Collecting distance is varied as 10, 15, and 20 cm.

of 10 cm results in flake-like nanofibers and a large diameter. Increasing the collecting distance improves fiber morphology, but some spindle-like fibers remain at 15 cm, and a relatively lower numbers of bead-like and spindle-like nanofibers were found at 20 cm. However, the diameter of nanofibers steadily decreases when the collecting distance was 20 cm.

At a PVA solution concentration of 10 wt.% (Figure 4 column (b)), a collecting distance of 10 cm results in a large variation in nanofiber diameter, as well as the formation of droplets/beads on nanofibers. The extent of this phenomenon is reduced when collecting distance is increased from 15 cm to 20 cm. Figure 4, column (c) shows the morphology of nanofibers with a specified PVA solution of 12 wt.% and different collecting distances. The beaded nanofiber structure is observed at a 10 cm collecting distance. Although the beaded morphology is improved to produce spindle-like and then fiber-like morphology as a result of increasing the collecting distance from 15 cm to 20 cm, the nanofibers are still not optimally formed.

In summary, the incorporation of a cylinder electrode into electrospinning can manipulate nanofiber morphology via different combinations of polymer concentration and collecting distance. Moreover, previous research indicates that the use of a wire electrode for electrospinning requires a relatively

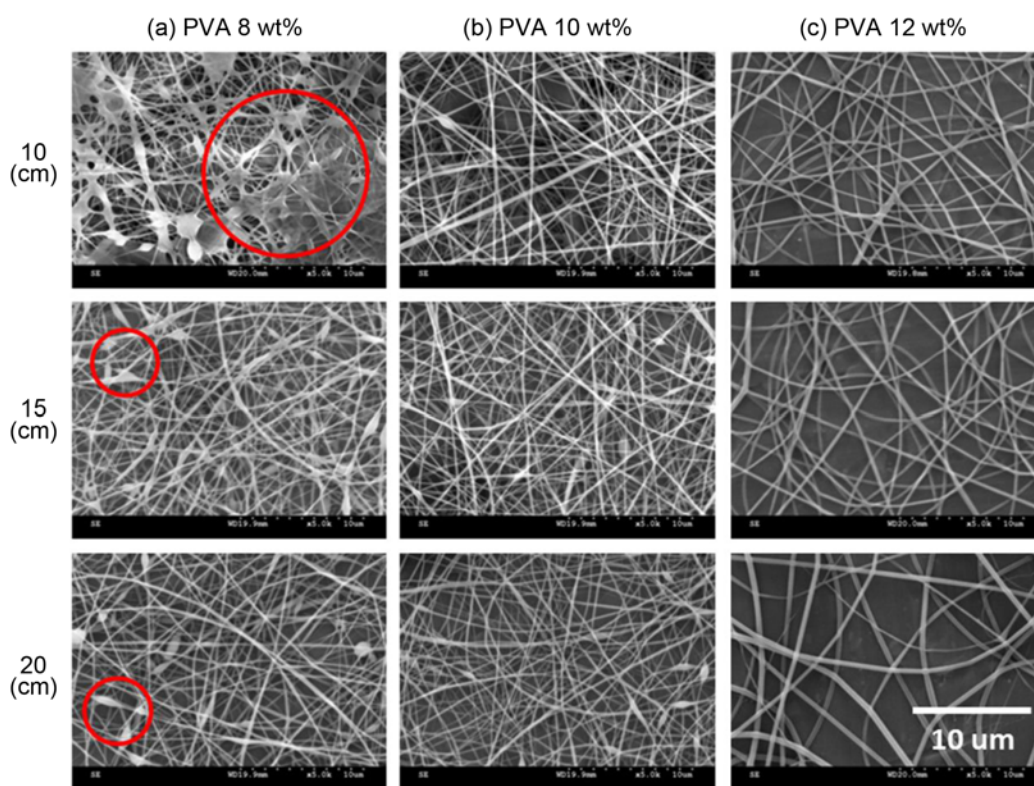
lower threshold voltage, as well as facilitates and improves electrospinning nanofibers to produce the desired morphology [29,30]. Therefore, we use different numbers of stainless steel wires as wire electrodes for electrospinning in the following discussion.

Table 2 shows the variations of nanofibers made using a cylinder electrode. Columns refer to PVA solution concentration (8, 10, and 12 wt.%), and the rows refer to collecting distance (10, 15, and 20 cm). With a specified 8 wt.% PVA concentration, the diameters with the corresponding collecting distances are  $1158\pm345$  (10 cm),  $946\pm181$  (15 cm), and  $534\text{ nm}\pm130\text{ nm}$  (20 cm). Moreover, for a specified 10 or 12 wt.% PVA concentration, the diameters are  $695\pm160/535\pm134$  (10 cm),  $654\pm158/624\pm138$  (15 cm), and  $593\text{ nm}\pm141\text{ nm}/640\text{ nm}\pm120\text{ nm}$  (20 cm).

The previous discussion of Figure 4 indicates that increasing collecting distance negatively influences nanofiber diameter. A larger collecting distance results in lower electric field force [24]. In this case, electrospinning does not apply the same amount of drawing force to nanofibers, thereby consequently resulting in a large range of nanofiber diameters. Furthermore, Table 2 shows that using a cylinder electrode requires a higher voltage to ensure that the polymer solution completely covers the cylinder, thereby resulting in a loss of voltage and an uneven drawing force for electrospinning.

**Table 2.** Diameter of PVA nanofiber (in nm) in relation to PVA concentration, collection distance, and number of SS twists

	PVA content (wt%)								
	8			10			12		
	Collection distances (cm)								
	10	15	20	10	15	20	10	15	20
Cylinder electrode	1158±345	946±181	534±130	695±160	654±158	593±141	535±134	624±138	640±120
1-SS	178±45	187±43	194±42	173±29	182±38	182±34	225±36	256±39	376±59
2-SS	186±33	168±41	189±45	95± 22	199±28	179±40	180±60	268±80	228±48
3-SS	91±22	87±20	112±36	138±40	130±38	152±52	302±67	262±83	215±67
4-SS	163±37	183±47	285±52	197±37	268±64	257±47	297±79	373±93	293±78

**Figure 5.** SEM images (5000 $\times$ ) of nanofibers that are electrospun with a 1-SS wire electrode; (a) 8, (b) 10, and (c) 12 wt.% PVA solutions and a collection distance of 10, 15, and 20 cm.

When PVA solution adheres to the cylinder electrode, it forms a wavy surface that interferes with the evenness of Taylor cones. Thus, the formed nanofibers have a broad range of diameter.

#### Morphology of PVA Nanofiber in Relation to the Number of SS Twists

Figure 5 indicates the SEM images of nanofibers that are electrospun with a 1-SS electrode. First, numerous droplet-like nanofibers were observed at a PVA solution concentration of 8 wt.% and collection distance of 10 cm. An increasing collection distance is conducive to better nanofiber morphology. However, some spindle-like fibers remain. The interlacing

points of fibers appear at a 15 cm collection distance, and bead-like and spindle-like fibers are present at a 20 cm collection distance.

Moreover, the nanofibers are made of 10 wt.% PVA. When the collection distance is 10 cm, the distribution area is wider, and droplets and beads are found over the nanofiber surface. At a collection distance of 15 cm, droplets are non-existent on the nanofibers, but some spindle-like fibers are found. These spindle-like fibers decrease as a result of a 20 cm collection distance.

In addition, a combination of a 12 wt.% PVA solution and a 10 cm collection distance results in the formation of a beaded structure in nanofibers. When the collection distance

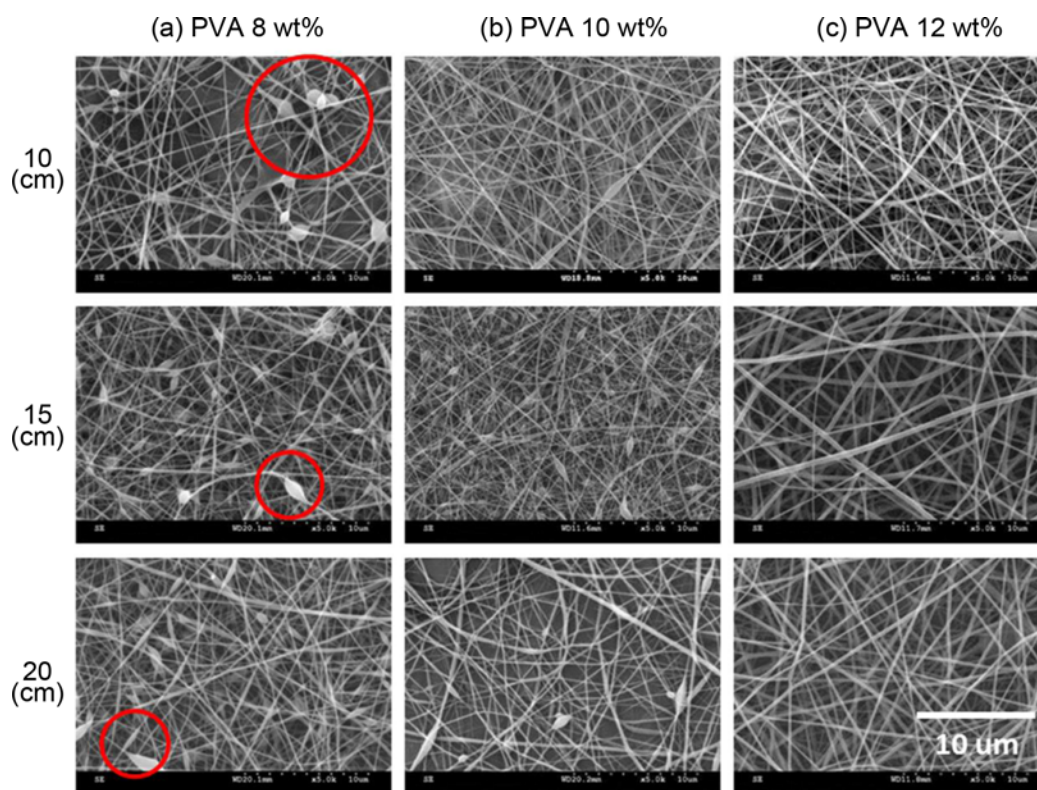
is increased, polymer solution is drawn to form spindle-like nanofibers with poor morphology. Regardless of collection distances, 12 wt.% PVA concentration can cause different diameters. This result is due to a significant increase in viscosity or the solidification of polymer solutions. In summary, nanofibers are formed in a sequence of droplets, beads, and spindles, and normal fiber morphology results from an increase in PVA concentration. Based on the microscopic view, nanofibers present a smooth morphology when produced in high PVA solution concentration. A high PVA concentration also facilitates the entanglement of molecular chains. Therefore, nanofibers are formed from bead-like to spindle-like, and the diameter of nanofibers gradually becomes even and larger. Excessive PVA concentration results in a broader diameter range. In addition, nanofibers present poor fibreizability because of insufficient distance between the spinneret and the collector. Collection distance prevents volatility of the PVA solution as solvent before being drawn to collectors as a result of a high electrostatic force, and results in droplets on nanofibers. Conversely, long collection distance causes a low electrostatic force that allows for longer solvent volatility duration, as exemplified by microscopic views. In other words, a long collection distance decreases the amount of droplet-containing and spindle-like nanofibers.

Table 2 shows the diameters of the electrospun nanofibers. An 8 wt.% PVA concentration results in diameters with

corresponding collection distances of  $178\pm 45$  (10 cm),  $187\pm 43$  (15 cm), and  $194\text{ nm}\pm 42\text{ nm}$  (20 cm). A 10 wt.% PVA concentration results in diameters with the corresponding collection distances of  $173\pm 29$  (10 cm),  $182\pm 38$  (15 cm), and  $182\pm 34$  nm (20 cm). Finally, 12 wt.% of PVA concentration results in diameters with the corresponding collection distances of  $225\pm 36$  (10 cm),  $256\pm 39$  (15 cm), and  $376\text{ nm}\pm 59\text{ nm}$  (20 cm).

In conjunction with a 1-SS wire electrode in electrospinning, the diameter of nanofibers is proportional to the collection distance. Longer collection distance results in a weak electrical field force, which consequently draws nanofibers with uneven diameters. With a specified collection distance of 20 cm, higher PVA concentration results in a wider space between nanofibers on the collector, as exemplified in Figure 4. PVA concentration is proportional to PVA viscosity. Longer collection distance does not facilitate electrospinning, and at the same time, causes uneven diameters of nanofibers.

The SEM images of nanofibers that are produced by using a 2-SS wire electrode are indicated in Figure 6. First, nanofibers produced in an 8 wt.% PVA solution are a collection of droplets and spindles with a collecting distance of 10 cm. The nanofibers are then transformed from beads to spindles as a result of a 15 cm collection distance. Nanofiber morphology is improved following increasing collection distance, and several spindle-like fibers were observed, or



**Figure 6.** SEM images (5000 $\times$ ) of nanofibers that are electrospun by incorporating a 2-SS wire electrode and (a) 8, (b) 10, and (c) 12 wt.% PVA solutions. Collection distances are 10, 15, and 20 cm.

nanofibers exhibit greater formability. A longer collection distance allows the solvent to fully evaporate, thereby decreasing the occurrence of droplet-like nanofibers. However, a longer collection distance also attenuates electrostatic attraction, which in turn provides lower electrostatic force to draw the polymer solution. Therefore, the unstable jets subsequently create a messy morphology of nanofibers.

Moreover, the combination of 10 wt.% PVA solution and a 10 or 15 cm collection distance also result in beads and spindles over nanofibers, being improved with a collection distance of 20 cm. In addition, the beaded structure and spindles disappear as a result of the combination of a 12 wt.% PVA solution. Small droplets appear over nanofibers with a collection distance of 10 cm, but the nanofibers already possess good morphology. A longer collection distance (such as 15 or 20 cm) further contributes to a smooth nanofiber surface that is devoid of beaded or spindle structures.

In summary, increasing PVA concentration decreases the formation of a beaded structure and a spindle-like morphology for nanofibers. This result is ascribed to the fact that a higher PVA concentration causes higher viscosity. With proper viscosity of the PVA solution and appropriate collection distance, electrostatic force induces jets that are smoothly drawn to the collector and form nanofibers with good morphology. Comparing Figures 5 and 6, a 2-SS wire

electrode provides nanofibers with better morphology compared with a 1-SS wire electrode. The twists formed by the SS wires enable the adhering PVA solution to overcome surface tension, thereby facilitating the jets to rapidly form nanofibers. In addition, an appropriate distance allows the solvent to fully evaporate and is thus conducive for the creation of morphology.

Table 2 illustrates the diameters of nanofibers that are electrospun by using a 2-SS wire electrode. An 8 wt.% PVA solution results in diameters with the corresponding collection distances of  $186\pm33$  (10 cm),  $168\pm41$  (15 cm), and  $189\text{ nm}\pm45\text{ nm}$  (20 cm). A 10 wt.% PVA solution causes diameters with corresponding collection distances of  $95\pm22$  (10 cm),  $119\pm28$  (15 cm), and  $179\text{ nm}\pm40\text{ nm}$  (20 cm). A 12 wt.% PVA solution yields diameters with the corresponding collection distances of  $179\pm60$  (10 cm),  $268\pm80$  (15 cm), and  $227\text{ nm}\pm48\text{ nm}$  (20 cm).

In summary, with the incorporation of a 2-SS wire electrode in electrospinning, nanofibers show diameters that increased and then decreased with longer collection distance. The wire electrode is activated by a disk, and less PVA solution adheres to its interlacing points because of the surface tension of the solution. As a result, small Taylor cones are formed when a high voltage is applied, and the diameter of nanofibers thus decreases. According to the test

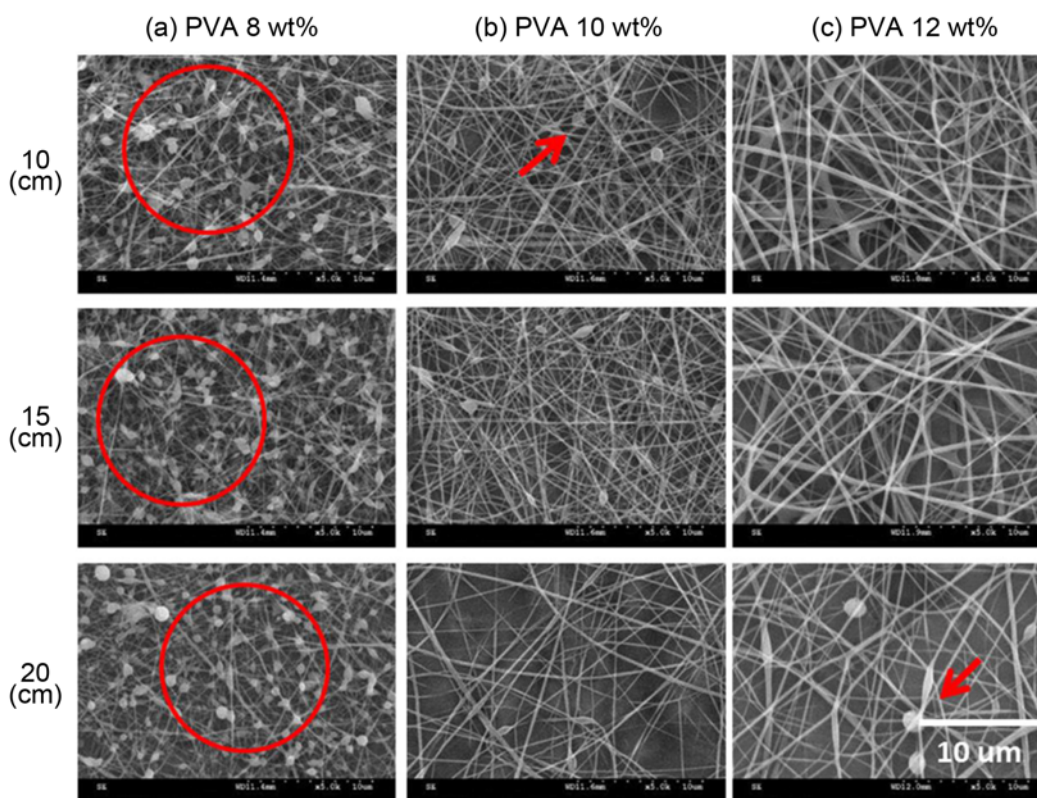


**Figure 7.** SEM images (5000 $\times$ ) of nanofibers that are electrospun by incorporating a 3-SS wire electrode and (a) 8, (b) 10, and (c) 12 wt.% PVA solutions. Collection distances are 10, 15, and 20 cm.

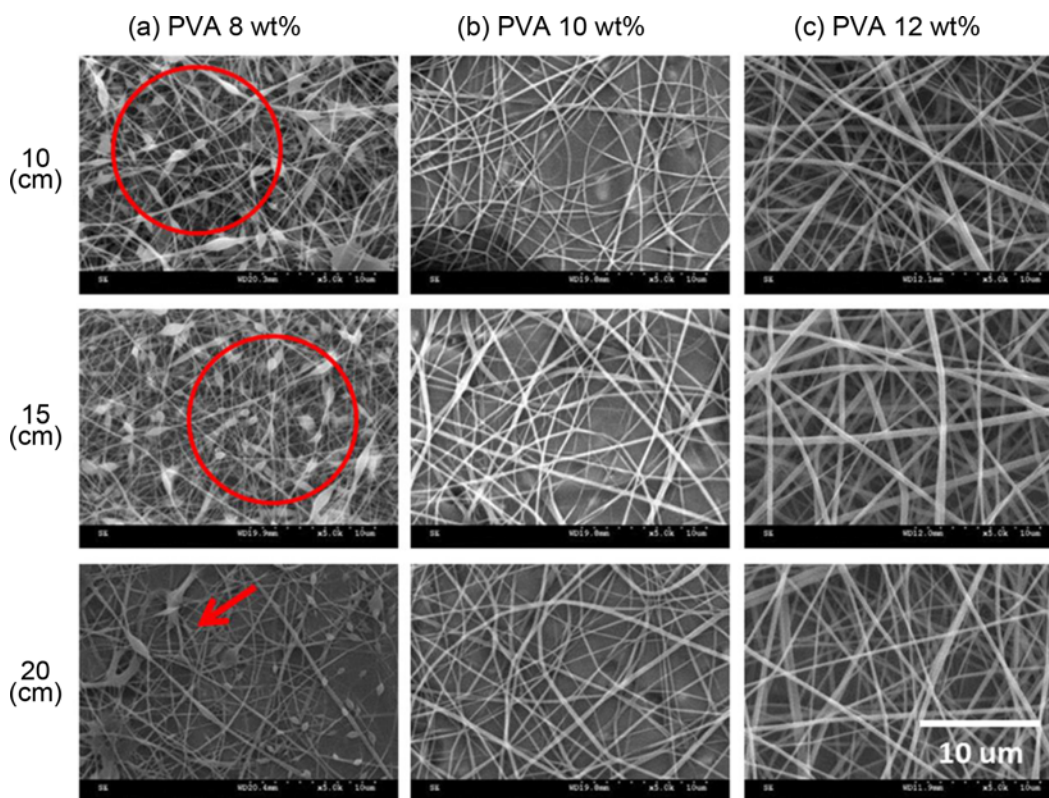
results, an optimal distribution of nanofibers occurs when the parameters are 12 wt.% PVA solution and a 20 cm collection distance.

Figure 7 illustrates the SEM images of nanofibers that are electrospun by using a 3-SS wire electrode. Regardless of collection distance, nanofibers that are electrospun in an 8 wt.% PVA solution are constructed with beads that fail to be drawn into nanofibers. The combination of a 10 wt.% PVA solution and a collection distance of 10 or 15 cm results in the required morphology of nanofibers with low amounts of beads. This morphology is improved with a longer collection distance; with an increased collection distance to 20 cm, the electrical field force decreases and results in a wider diameter range of nanofibers.

In addition, nanofibers that are made of a combination of a 12 wt.% PVA solution and a 10 cm collection distance possess a wide range of diameter, but their beaded structure is improved. The morphology is uneven and appears messy when collection distance is increased.

In summary, when using a 3-SS wire electrode for electrospinning, collection distance exerts a distinct influence on nanofiber morphology. In particular, regardless of PVA concentrations, a 20 cm collection distance causes lower electrical field force that creates a wide range of diameter and messy morphology of nanofibers.

Table 2 indicates the diameter of nanofibers that are electrospun with a 3-SS wire electrode. The diameters of nanofibers that are made in an 8 wt.% PVA solution along with the corresponding collection distances are  $91\pm 22$  (10 cm),  $87\pm 20$  (15 cm), and  $112\text{ nm}\pm 360\text{ nm}$  (20 cm). The diameters of nanofibers made in 10 wt.% PVA solution along with the corresponding collection distances are  $138\pm 40$  (10 cm),  $130\pm 38$  (15 cm), and  $152\text{ nm}\pm 52\text{ nm}$  (20 cm). The diameters of nanofibers that are made in 12 wt.% PVA solution along with the corresponding collection distances are  $302\pm 67$  (10 cm),  $262\pm 83$  (15 cm), and  $215\text{ nm}\pm 67\text{ nm}$  (20 cm). With a 3-SS wire electrode, the nanofibers yield a wide range of diameters as a result of increasing PVA concentrations. High concentration equally means high viscosity. The PVA solution adhering to the interlacing points of the wire electrode forms spheres with different sizes and eventually results in uneven diameters of the nanofibers, especially for nanofibers that are made in 12 wt.% PVA solution. Figure 8 shows nanofibers that are electrospun by incorporating a 4-SS wire electrode. First, an 8 wt.% PVA solution forms spindle-like nanofibers at a collection distance of 10 or 15 cm and then forms a non-fibrous morphology when collection distance is increased to 20 cm. These results suggest that morphology does not depend on collection distances. Moreover, a 10 wt.% PVA



**Figure 8.** SEM images (5000 $\times$ ) of nanofibers that are electrospun by incorporating a 4-SS wire electrode and (a) 8, (b) 10, and (c) 12 wt.% PVA solutions. Collection distances are 10, 15, and 20 cm.



solution yields nanofibers without the beaded structure, regardless of collection distances. This morphology is not improved by increasing the collection distance to 20 cm. In addition, a 12 wt.% PVA concentration contributes to the improvement in nanofiber morphology, but with a wide range of diameters. A combination of 12 wt.% PVA solution and a 10 cm collection distance results in fine nanofibers. The nanofibers turn into fibrous status, but with a wide diameter range.

In summary, the morphology of nanofibers is highly correlated with the increase in PVA concentration. Collection distance can slightly improve the morphology. With a specified 12 wt.% PVA concentration, increasing collection distance results in a wide range of nanofiber diameters. One possible cause is that a wire electrode that is formed by twisting four stainless steel wires possesses a rugged surface. During electrospinning, the PVA solution adhering to the wire electrode is turned into spheres at various sizes because of gravity, surface tension, and viscosity. The differently sized spheres are thus formed as differently sized Taylor cones that eventually provide nanofibers with different diameters.

Table 2 shows the diameters of nanofibers that are produced by incorporating a 4-SS wire electrode. The diameters of nanofibers that are made in 8 wt.% PVA solution along with the corresponding collection distances are 163±37 (10 cm), 163±37 (15 cm), and 285 nm±52 nm (20 cm). The diameters of nanofibers that are made in 10 wt.% PVA solution along with the corresponding collection distances are 197±37 (10 cm), 268±64 (15 cm), and 257 nm±47 nm (20 cm). The diameter of nanofibers that are made in 12 wt.% PVA solution along with the corresponding collection distances are: 297±79 (10 cm), 373±93 (15 cm), and 293 nm±78 nm (20 cm). Moreover, 3-SS and 4-SS twist also results in greater crossing points of the wire electrode, which prevents PVA solution from forming Taylor cones, and eventually the diameter of nano-fibers is uneven. This result indicates an inversely proportional relationship between the diameter of nanofibers and the amount of stainless steel wires that comprise the wire electrode.

### Conclusion

This study has proven that nanofibers formed using a wire electrode present a more even morphology than those formed using a cylinder electrode. The test results indicate that nanofibers can yield good morphology with the incorporation of a 10 wt.% PVA solution. Increasing the collection distance from 10 cm to 20 cm slightly improves the morphology of nanofibers, whereas an increase in PVA concentration is highly correlated with the morphology and diameters of nanofibers. Moreover, using 2-SS twist as a wire electrode results in an optimal morphology of nanofibers. In future studies, we suggest that wire electrodes should be

created by synthesizing various materials, and the influences on the formability and production efficiency of the resulting nanofibers should be studied.

### Acknowledgements

The authors would especially like to thank Ministry of Science and Technology of the Taiwan, for financially supporting this research under Contract MOST 103-2622-E-166-001-CC2. Dr. Jia-Horng Lin and Dr. Yueh-Sheng Chen contributed equally to this work.

### References

1. R. Nirmala, D. Kalpana, J. W. Jeong, H. J. Oh, J.-H. Lee, R. Navamathavan, Y. S. Lee, and H. Y. Kim, *Colloid. Surf. A: Physicochem. Eng. Asp.*, **384**, 605 (2011).
2. X. Hu, S. Liu, G. Zhou, Y. Huang, Z. Xie, and X. Jing, *J. Control. Release*, **185**, 12 (2014).
3. H. Zhang, S. Li, C. J. Branford White, X. Ning, H. Nie, and L. Zhu, *Electrochim. Acta*, **54**, 5739 (2009).
4. Y. Liu, R. Wang, H. Ma, B. S. Hsiao, and B. Chu, *Polymer*, **54**, 548 (2013).
5. A. Cooper, R. Oldinski, H. Ma, J. D. Bryers, and M. Zhang, *Carbohydr. Polym.*, **92**, 254 (2013).
6. Y.-L. Huang, A. Baji, H.-W. Tien, Y.-K. Yang, S.-Y. Yang, S.-Y. Wu, C.-C. M. Ma, H.-Y. Liu, Y.-W. Mai, and N.-H. Wang, *Carbon*, **50**, 3473 (2012).
7. F. Anton, *U. S. Patent*, 1975504 (1934).
8. D. Li and Y. Xia, *Adv. Mater.*, **16**, 1151 (2004).
9. W. S. Khan, R. Asmatulu, M. Ceylan, and A. Jabbarnia, *Fiber. Polym.*, **14**, 1235 (2013).
10. J. He, L. Wang, R. Liu, M. Zhang, W. Tan, and Y. Wu, *Fiber. Polym.*, **15**, 2283 (2014).
11. D. Nurwaha and X. Wang, *Fiber. Polym.*, **16**, 850 (2015).
12. A. Valipouri, S. A. H. Ravandi, and A. R. Pishevar, *Fiber. Polym.*, **14**, 941 (2013).
13. X. Wang, T. Lin, and X. Wang, *Fiber. Polym.*, **15**, 961 (2014).
14. F. Cengiz-Çallioğlu, O. Jirsak, and M. Dayik, *Fiber. Polym.*, **13**, 1266 (2012).
15. H. Niu and T. Lin, *J. Nanomater.*, **2012**, 12 (2012).
16. G. Jiang, S. Zhang, and X. Qin, *Mater. Lett.*, **106**, 56 (2013).
17. H. Niu, T. Lin, and X. Wang, *J. Appl. Polym. Sci.*, **114**, 3524 (2009).
18. X. Wang, X. Hu, X. Qiu, X. Huang, D. Wu, and D. Sun, *Mater. Lett.*, **99**, 21 (2013).
19. F.-L. Zhou, R.-H. Gong, and I. Porat, *J. Mater. Sci.*, **44**, 5501 (2009).
20. C. Huang, H. Niu, C. Wu, Q. Ke, X. Mo, and T. Lin, *J. Biomed. Mater. Res. Part A*, **101**, 115 (2013).
21. D. Wu, X. Huang, X. Lai, D. Sun, and L. Lin, *J. Nanosci. Nanotechnol.*, **10**, 4221 (2010).
22. A. L. Yarin and E. Zussman, *Polymer*, **45**, 2977 (2004).

23. J. Chaloupek, O. Jirsak, V. Kotek, D. Lukas, L. Martinova, and F. Sanetnik, *U. S. Patent*, 7585437 (2005).
24. Y. Liu and J.-H. He, *Int. J. Nonlin. Sci. Num.*, **8**, 393 (2007).
25. Y. Liu, J.-H. He, and J.-Y. Yu, *J. Phys. Conf. Ser.*, **96**, 012001 (2008).
26. X. Wang, H. Niu, T. Lin, and X. Wang, *Polym. Eng. Sci.*, **49**, 1582 (2009).
27. X. Wang, H. Niu, X. Wang, and T. Lin, *J. Nanomater.*, **2012**, 3 (2012).
28. T. Lin, X. Wang, X. Wang, and H. Niu, *W.O. Patent*, 2010043002 A1 (2011).
29. K. M. Forward and G. C. Rutledge, *Chem. Eng. J.*, **183**, 492 (2012).
30. I. Bhattacharyya, M. C. Molaro, R. D. Braatz, and G. C. Rutledge, *Chem. Eng. J.*, **289**, 203 (2016).
31. H. Itoh, Y. Li, K. H. K. Chan, and M. Kotaki, *Polymer Bull.*, DOI:10.1007/s00289-016-1620-8 (2016).
32. H. Jani, P. Toni, S. Eero, and R. Mikko, *Nanotechnology*, **26**, 025301 (2015).
33. S. L. Liu, Y. Y. Huang, H. D. Zhang, B. Sun, J. C. Zhang, and Y. Z. Long, *Mater. Res. Innov.*, **18**, S4 (2014).
34. X. Wang, X. Wang, and T. Lin, *J. Mater. Res.*, **27**, 3013 (2012).
35. Z.-M. Huang, Y. Z. Zhang, M. Kotaki, and S. Ramakrishna, *Compos. Sci. Technol.*, **63**, 2223 (2003).
36. X. Zong, K. Kim, D. Fang, S. Ran, B. S. Hsiao, and B. Chu, *Polymer*, **43**, 4403 (2002).